Large anomalous Nernst coefficient in an oxide skyrmion crystal Chern insulator

Yo Pierre Mizuta and Hikaru Sawahata
Graduate School of Natural Science and Technology, Kanazawa University, Kanazawa, Ishikawa 920-1192, Japan

Fumiyuki Ishii*
Faculty of Mathematics and Physics, Kanazawa University, Kanazawa, Ishikawa 920-1192, Japan

(Received 27 March 2018; published 15 November 2018)

Our first-principles calculation predicts a sizable transverse thermoelectric coefficient N in a skyrmion crystal assumed on EuO monolayer. Such N arises from the coexistence of large longitudinal thermoelectric coefficient *and* large Hall angle ratio, realized in the vicinity of a band gap with Chern number $\mathcal{C} = 2$. This demonstrates a prototype of novel class of thermoelectric materials utilizing the topological texture of electronic spins, motivating further studies including relevant experiments.

DOI: 10.1103/PhysRevB.98.205125

I. INTRODUCTION

Thermoelectric (TE) conversion (generation of electric power from heat) offers us a way of reviving an enormous amount of waste heat, paving the way for a more energy-efficient society. One of the prerequisites for realizing such TE applications is to find materials with large enough TE coefficients, i.e., Seebeck (Nernst) coefficient S (N) quantifying a generated electric field $\mathbf{E}$ parallel (perpendicular) to the temperature gradient ∇T. While the Seebeck-based TE modules have been at the center of applied studies, the Nernst-based ones have various advantages over the former: simpler and more flexible structure that facilitates its fabrication and its application to heat sources with nonflat surfaces. The minimum $|N|$ for the latter to be useful was estimated to be $\sim$20 μV/K [1].

Nonzero N can appear in a material only when at least either of the transverse currents $j_x^{(\mathrm{H})} = \sigma_{xy} E_y$ or $j_x^{(\mathrm{N})} = \alpha_{xy} \nabla_y T$ is present, whose conductivities relate to the TE coefficients as described in Sec. II. It can be shown, for a two-dimensional system on the xy plane, that this condition requires breaking of both the time-reversal ($\mathcal{T}$) symmetry and the mirror ($\mathcal{M}$) symmetry with respect to planes normal to the xy plane. Such a situation is realized, obviously in the presence of an externally applied *real* magnetic field B_z^{ext}, but also in the presence of some field B_z^{int} that emerges from internal degree(s) of freedom of the material and possesses the same symmetry property as that of B_z^{ext}. The B_z^{int} in a crystalline material is generally identified to be the *Berry curvature* [2] $\boldsymbol{\Omega}(\boldsymbol{k}) \equiv i \langle \partial_{\boldsymbol{k}} u | \times | \partial_{\boldsymbol{k}} u \rangle$, defined in the space of the lattice periodic part of Bloch states $|\psi_{\boldsymbol{k}}\rangle = e^{i\boldsymbol{k}\cdot\hat{\boldsymbol{r}}} |u_{\boldsymbol{k}}\rangle$ parameterized with crystal momentum $\boldsymbol{k}$. In the presence of B_z^{ext}(B_z^{int}), the consequent emergence of $j_x^{(\mathrm{H})}$ and $j_x^{(\mathrm{N})}$ is called the ordinary (anomalous) Hall effect [OHE (AHE)] and the ordinary(anomalous) Nernst effect [ONE (ANE)], respectively. In terms of applications, the use of OHE and ONE, which involves the attachment of strong magnets to the TE converter, is not practically convenient, while the use of AHE and ANE is not yet realistic with the small values $|N| \lesssim 1 \mu\mathrm{V/K}$ of most of the materials so far investigated. Therefore the question of particular interest is: *How large could $|N|$ be by virtue of AHE and ANE?*

The necessary condition to obtain AHE and/or ANE in a given system can be satisfied through either of the following two scenarios: (i) $\mathcal{T}$-symmetry breaking due to a *coplanar* magnetic structure, combined with $\mathcal{M}$-symmetry breaking due to spin-orbit interaction [3,4] or (ii) simultaneous breaking of $\mathcal{T}$ and $\mathcal{M}$ symmetries due to a *noncoplanar* magnetic structure [5,6].

In this paper, we concentrate on (ii), and out of many possible noncoplanar patterns, particularly on the *skyrmion*, which has received special interests associated with its quantized (particlelike) nature [7]. We further limit ourselves to its crystalline form *skyrmion crystal* (SkX). Our previous work [8] predicted a surprisingly large ANE in a model of SkX whose AHE had been investigated by Hamamoto *et al.* [9], but the studied electronic structure was a very simple one. There being some experimental studies on the ANE in SkX [10,11] as well as many other studies on AHE, we now target a more realistic system made of EuO by taking advantage of large scale first-principles calculations. The choice of EuO is motivated by a recent experiment where skyrmionlike magnetic structure was implied [12]. The results show that SkX is indeed such a structure that can support large $|N|$.

This paper is organized as follows: In Sec. II, we present the expression of N (and also S) evaluated in this study and note a well-known simple relation between AHE and ANE, which is very instructive in the quest for larger $|N|$. In Sec. III, we describe the details of our EuO model, both its geometry and the choice of parameters. In Sec. IV, we summarize the employed computational procedure based on first-principles methods. Section V is the main part giving results and discussions on the electronic structure and consequent transport coefficients. The key finding was that our model becomes a *Chern insulator* [13] of *Chern number*

*ishii@cphys.s.kanazawa-u.ac.jp

$\mathcal{C} = 2$, which generates large $|N|$ when lightly doped with carriers, due to the coexistence of large Seebeck effect and large AHE.

II. EXPRESSIONS OF THERMOELECTRIC QUANTITIES

The formulas for the thermoelectric coefficients to be evaluated follow from the linear response relation of charge current: $\mathbf{j} = \tilde{\sigma}\mathbf{E} + \tilde{\alpha}(-\nabla T)$. Using the conductivity tensors $\tilde{\sigma} = [\sigma_{ij}]$ and $\tilde{\alpha} = [\alpha_{ij}]$, we obtain [8]

$$S \equiv S_{ii} \equiv \frac{E_i}{\nabla_i T} = \frac{S_0}{1+r_H^2} + \frac{r_H N_0}{1+r_H^2}$$
$$N \equiv S_{xy} \equiv \frac{E_x}{\nabla_y T} = \frac{N_0}{1+r_H^2} - \frac{r_H S_0}{1+r_H^2}. \quad (1)$$

Here we defined $S_0 \equiv \alpha_{xx}/\sigma_{xx}$ (*pure Seebeck coefficient*), $r_H \equiv \sigma_{xy}/\sigma_{xx}$ (*Hall angle ratio*), $N_0 \equiv \alpha_{xy}/\sigma_{xx}$ (*pure Nernst coefficient*) for a simpler notation. The first term in each of S and N, which is proportional to pure coefficient S_0 and N_0, respectively, survives in the vanishing AHE condition $r_H = 0$, while the second term is present only when $r_H \neq 0$. The sign relation among S_0, N_0, and r_H determines whether the two terms work constructively or destructively in each of the resultant S and N. In the presence of AHE and ANE ($r_H \neq 0,\ N_0 \neq 0$), the mixture of pure coefficients S_0 and N_0 gives the measured coefficients S and N.

Importantly, the AHE and ANE are related via a simple formula [14]. Particularly at low temperatures, where the chemical potential μ nearly matches the Fermi energy ε_F, it reduces to the well-known Mott relation:

$$\alpha_{ij}(T,\ \mu \simeq \varepsilon_F) \simeq \frac{\pi^2 k_B^2}{3e} \frac{d\sigma_{ij}(T=0,\varepsilon_F)}{d\varepsilon_F} T. \quad (2)$$

This instructs us to seek for $\sigma_{ij}(\varepsilon)$ that varies more rapidly at ε_F in order to achieve larger N_0.

III. MODEL

As a realistic material we choose EuO, which is a rare ferromagnetic insulator in bulk with half-filled $4f$ shells forming Heisenberg-type spins. We specifically consider its monolayer (two-dimensional limit). A 2D square unit cell is constructed on a (100) plane, with one of the FCC cell vectors (length $a/\sqrt{2}$) quadrupled in length chosen as one of the desired cell vectors. The lattice constant was set to $2\lambda \equiv (a = 5.14)/\sqrt{2} \times 4 = 14.54$ Å, adopting the bulk value as a [15].

As to the magnetic structure, we forced the spins of 16 Eu atoms within each cell to form a skyrmion equivalent to the one previously studied [9], i.e., the spin spherical coordinates vary according to $\theta(\boldsymbol{r}) = \pi(1 - r/\lambda)$ for $r < \lambda$ and $\theta = 0$ for $r > \lambda$, along with $\phi = \tan^{-1}(y/x)$. Note that this skyrmion structure is not the lowest energy solution within the density functional theory we employ. Nevertheless, since there is some trace of skyrmionlike objects in experiments [12], it should be meaningful to *assume* the structure and see the consequences, without stepping into the unclarified stabilizing mechanism.

An image of our unit cell is shown in Fig. 1. The noncoplanar $\{\theta(\boldsymbol{r}),\ \phi(\boldsymbol{r})\}$ gives rise to an emergent magnetic field

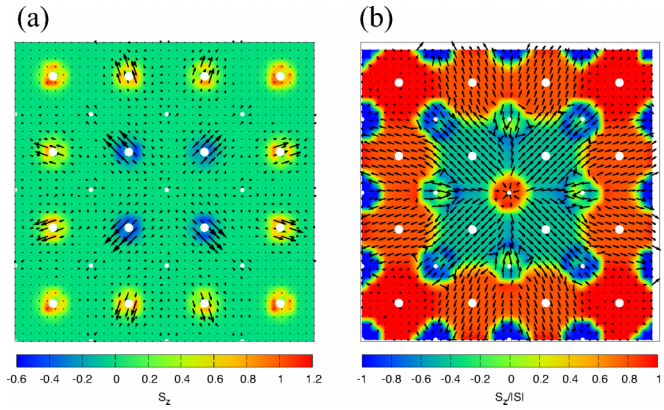

FIG. 1. (a) Spin momentum density $\boldsymbol{S}(\boldsymbol{r})$ evaluated from the wave functions on grid points. The out-of-plane component S_z is expressed with color, while the in-plane components are represented with black arrows. (b) A plot corresponding to the left one, but for normalized spin density $\boldsymbol{S}(\boldsymbol{r})/|\boldsymbol{S}(\boldsymbol{r})|$. Both panels illustrate a single square unit cell of 4×4 SkX, with the length of each side being 2λ. The Eu (O) atoms are indicated with large (small) white filled circles.

$B_{\text{spin}}(\boldsymbol{r}) = (\hbar/2e)(\pi/r\lambda)\sin\pi(1 - r/\lambda)$ [16], whose spatial average in a unit cell is $\overline{B}_{\text{spin}} = (h/e)/(\pi\lambda^2)$. Thus, the associated cyclotron frequency in our model is evaluated to be $\overline{\omega_s} = e\overline{B}_{\text{spin}}/m^* \approx 10^{14}$ s^{-1}, given the effective mass of $m^* \approx 0.3$ reported by Ref. [17].

Regarding the scattering effects on electrons, we adopt the constant-relaxation-time (τ) approximation (RTA) for expressing the distribution of electrons. While $\tau = m^* \times (\text{mobility} \approx 30\ \text{cm}^2\ \text{V}^{-1}\ \text{s}^{-1})/e \approx 100$ fs is roughly estimated from the experimentally inferred mobility [12], we will consider three different values of $\tau = 10$ fs, 100 fs, 1 ps, since we can expect τ to vary substantially depending on the sample details. Correspondingly, electrons can typically complete as many as $(\overline{\omega_s}\tau)/(2\pi)$ cycles between successive scattering events, with $\overline{\omega_s}\tau \approx 1,\ 10,\ 100$. Since the Berry-curvature-driven σ_{xy} we evaluate here is well defined for $\overline{\omega_s}\tau \gg 1$, the choice of larger two values seems sound.

IV. COMPUTATIONAL PROCEDURE

Our calculations consist of three steps: (1) Obtaining the electronic states of target SkX using OPENMX [18], (2) constructing Wannier functions employing WANNIER90 [19], and finally (3) computing all the necessary transport quantities [tensors σ and α in Eq. (1)] in the obtained Wannier basis using a postprocessing code POSTW90 [20].

In step (1), the calculation was performed based on the density functional theory within Perdew-Burke-Ernzerhof's generalized gradient approximation (GGA) of exchange-correlation energies, including a Hubbard U correction of $U = 6.0$ eV for the localized Eu-f orbitals. Norm-conserving pseudopotentials were used, and a set of pseudoatomic orbital basis was specified as Eu8.0-$s2p2d2f1$ and O5.0-$s2p2d1$, where the number after each element standing for the radial cutoff in the unit of bohr, and the integer after s, p, d, f indicating the radial multiplicity of each angular momentum component. Cutoff energy of 300 Ry for the charge density and a k-points grid of $4 \times 4 \times 1$ were adopted.

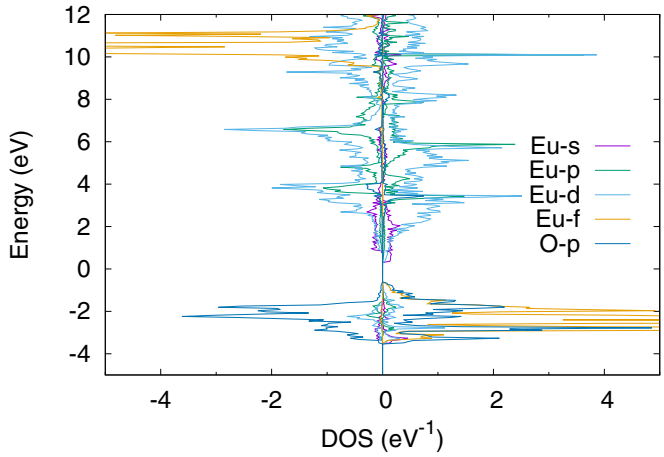

FIG. 2. Spin-, atom-projected density of states of collinear ferromagnetic EuO monolayer in a broad range of energy.

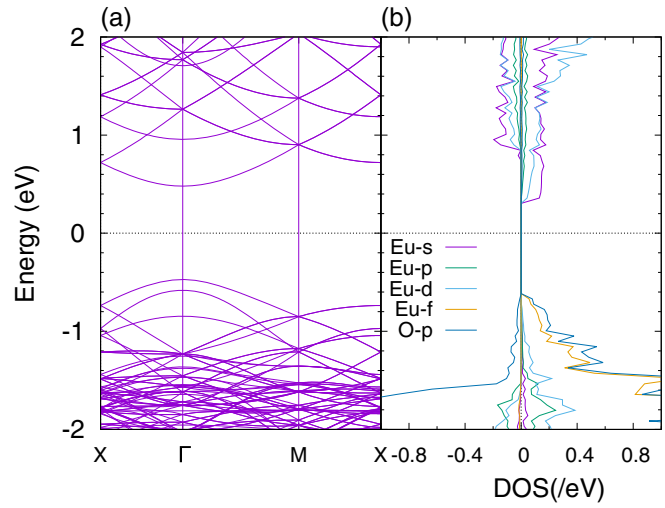

FIG. 3. (a) Band structure and the (b) spin-projected density of states for the FM system, focused around the Fermi energy.

In step (2), from a total of 214 bands falling inside the energy window of [0,10] eV, 192 Wannier orbitals were extracted starting from the projection of a set of (s, d)-character localized orbitals on Eu sites onto the original Bloch states sampled on a k grid of $4 \times 4 \times 1$. The states inside [0,3] eV were frozen during the extraction process, so that the original band dispersion was maintained as is required for the exact evaluation of σ_{xx} and α_{xx} and for a reasonable evaluation of σ_{xy} and α_{xy}.

In step (3), all the conductivities were evaluated within RTA to the semiclassical Boltzmann transport theory [21], where the numerical integrations in k space were performed on a grid of $100 \times 100 \times 1$. In addition to the above energy-decomposed analysis, we have also performed band-by-band identification of Chern number C_n (n: band index), in the aim of clarifying the topological structure of the electronic bands.

V. RESULTS AND DISCUSSIONS

A. Basic results

Let us first look at the landscape of spin momentum density obtained after the self-consistent calculation. As shown in Fig. 1(a), large momentum is strongly localized around Eu atoms, which justifies the ionic picture of Eu-4f shell. Furthermore, its directional distribution in the vicinity of Eu atoms, nicely radiating from the unit cell center, is scarcely changed from the initial setting of our skyrmion texture described in Sec. III, suggesting the spin-constraining method in OPENMX worked effectively during the self-consistent process. It is also interesting to pay attention to the directional distribution in the inter-Eu region: Closer inspection of the normalized spin density vector drawn in Fig. 1(b) reveals the strongly antiferromagnetic nature of the coupling between Eu and O atoms, although the latter have much smaller ($<0.2\ \mu_B$) momentum.

Before discussing the electronic structure of the SkX, we look at the density of states (DOS) of collinear ferromagnetic (FM) state in a broad range of energy as shown in Fig. 2. It was confirmed to be reasonable with the choice of $U = 6.0$ eV, in the sense that the position of the Eu-f levels roughly 2 eV below the conduction band bottom is consistent with what had been obtained from the all-electron method for bulk EuO [22]. Perfect polarization of Eu-f spins ($\sim 7\ \mu_B$) is indicated, while those states are absent in the range of 10 eV from the conduction band bottom, where Eu-s, -p, -d states are dominant.

B. Effects of SkX on electronic structure

Hereafter we focus on the lower energy region of Fig. 2, whose enlarged DOS and band dispersion are shown in Fig. 3. The corresponding plots for the SkX system are in Fig. 4. While bands are degenerate on symmetry points or lines in the FM case, they become gapped once the spins form SkX. This can be understood as a consequence of symmetry lowering due to the appearance of emergent magnetic field $B_z^{\rm int}$, with the periodicity enlarged from that in the FM state.

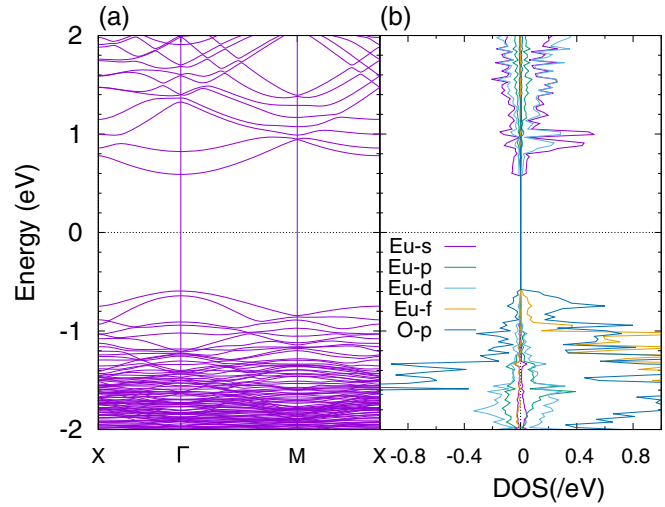

FIG. 4. (a) Band structure and (b) the spin-projected density of states for the SkX system, focused around the Fermi energy.

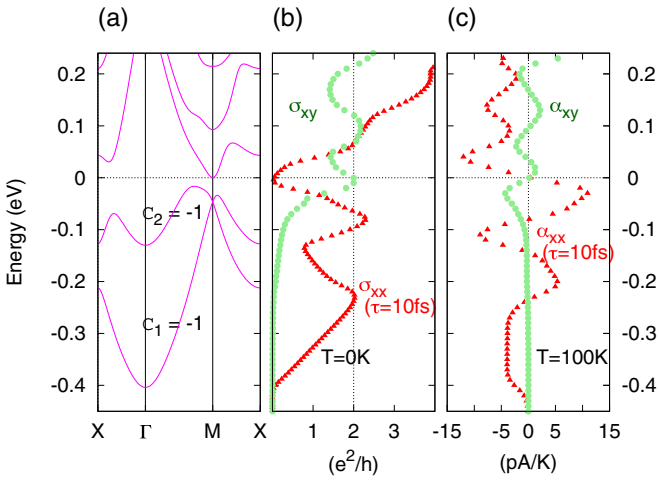

FIG. 5. (a) Zoomed-in band structure around the conduction band bottom, and the chemical potential dependence of (b) zero-temperature electric conductivities $\sigma_{xx}(\tau = 10$ fs) and σ_{xy}, and of (c) thermoelectric conductivities $\alpha_{xx}(\tau = 10$ fs) and α_{xy} at 100 K. The system has two additional electrons as compared to the pristine system, which occupy the lowest two bands in (a), where their respective Chern numbers of -1 are indicated. A Gaussian smearing of 10 meV is employed for (b).

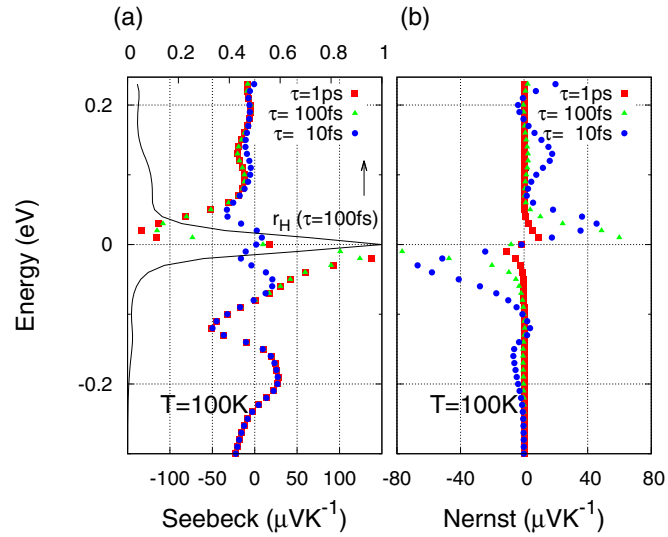

FIG. 6. Chemical potential dependence of TE coefficients: (a)S and (b)N at 100 K, respectively. Results are shown for three different values of τ in each case. Additionally, the Hall angle ratio r_H for $\tau = 100$ fs is plotted on the second axis in (a) [black solid line].

Consequently, the bands become narrower, exhibiting many local gaps (anticrossings), and accordingly the DOS shows more ups-and-downs in SkX than in FM. Particularly, there is a global (equienergy) gap of ∼20 meV between the second and the third band (counted from the conduction band bottom). This band structure is a realistic example of a Landau level which is split and dispersed by crystal potential, so far reported in tight-binding models under a uniformly applied magnetic field [23] or a SkX-driven inhomogeneous emergent field [9,24], the latter sharing the same physical origin as ours.

A clear evidence of emergent magnetic field in our system is the nonzero Chern numbers we obtained, for example $C_1 = C_2 = -1$ (labeling the conduction bands as 1, 2,... from the bottom) [Fig. 5]. This is consistent with earlier observations, based on Onsager's semiclassical-quantization argument, that the Chern number roughly corresponds to the number of topologically disconnected Fermi surfaces of the original bands in the absence of magnetic field [23,24]: In fact, in the energy range of $n = 1, 2$ bands, there is only one electron pocket around Γ point in the absence of SkX structure, i.e., when the bands of FM EuO shown in Fig. 3(a) are unfolded to the primitive Brillouin zone.

An important finding here is that our SkX becomes a Chern insulator of $\mathcal{C} = 2$ when it is doped with two additional electrons per SkX unit cell (0.125 electron per Eu atom), filling the bands $n = 1,\ 2$. This was already implied in the pristine system (Fig. 4) and indeed confirmed by an explicit self-consistent calculation including two additional electrons (Fig. 5). With the Fermi energy located inside the previously mentioned global gap of ∼20 meV, the Hall conductivity is quantized to be $\sigma_{xy} = 2(e^2/h)$ in the insulating phase ($\sigma_{xx} = 0$) [Fig. 5(b)].

C. Thermoelectric response largely modulated by SkX

Now we will discuss our main subjects, the thermoelectric quantities of the system, firstly focusing on a fixed temperature $T = 100$ K, which is below the highest Curie temperatures T_c of EuO systems, so far reported in La-doped thin films [25]. The computed Seebeck/Nernst coefficients are shown in Fig. 6 for three different strengths of disorder parametrized by a relaxation time $\tau = 10$ fs, 100 fs, 1 ps.

Our principal result is a large N expected for a moderate value of $\tau = 100$ fs, reaching its peak of $N \approx 20\ \mu$V/K at $\mu \simeq 30$ meV, which becomes an order of magnitude smaller for $\tau = 1$ ps. This is in contrast to $|S|$, which is about five times larger than N at that μ for $\tau = 100$ fs and remains almost the same for ten times longer τ. To understand such behavior of S and N, we pay attention to the magnitude of r_H and the sign relation among S_0, N_0, and r_H. In the following we focus on around $\mu \sim \pm 30$ meV [26], as well as on the choice of $\tau \geqslant 100$ fs for the reason stated at the end of Sec. III.

Firstly, we find from Fig. 6(a) that $r_H(\mu = \pm 30\ \text{meV}) \lesssim 0.2$ for $\tau \geqslant 100$ fs. In this case, the expression Eq. (1) can be approximated up to the error of $\lesssim 5\%$ as $S \simeq S_0 + r_H N_0$ and $N \simeq N_0 - r_H S_0$. They can be further approximated as

$$S \simeq S_0, \text{ and } N \simeq -r_H S_0, \tag{3}$$

since the peaks in question satisfy $|S_0| \gtrsim (20 \sim 100) \times |N_0|$ [as understood by comparing the red points multiplied by a number >10 (corresponding to $\tau \geqslant 100$ fs) and the green points in Fig. 5(c)].

We thus recognize from Eq. (3), importantly, that the large $|N|$ is due to the combination of large Seebeck effect $\propto S_0$ and large AHE $\propto r_H$. Moreover, the above-mentioned τ dependence is naturally understood, considering the properties $r_H \propto \tau^{-1}$ and $S_0 \propto \tau^0$.

Regarding the variation of temperature (not shown in the figure), it was found that the maximum of $|N|$ in the energy

TABLE I. Some limiting cases leading to large $|N|$ when $r_H^2 \ll 1$.

	Condition	Typical patterns for $\lvert N\rvert > 10\ \mu$V/K N	$\lvert S_0\rvert$	$\lvert r_H\rvert$	$\lvert N_0\rvert$	
I	$\lvert N_0\rvert \ll r_H S_0$	$\sim -r_H S_0$	$>10^3$	$\sim 10^{-2}$		(a)
			$>10^2$	$\sim 10^{-1}$		(b)
II	$\lvert N_0\rvert \gtrsim r_H S_0$	$\sim N_0$			>10	(c)

range of Fig. 6 is $\approx 10\mu$V/K at $\mu \simeq \pm 30$ meV at 300 K [27], about half the value discussed above at the same μ at 100 K. This suppression of N on heating was found to be due to the decline of both r_H and $|S_0|$. The decline of $|S_0|$ immediately shows that the Mott's relation (low T approximation) $S_0 \propto T$ is not respected between these temperatures. This is roughly attributed to the narrowness of the gap ≈ 20 meV [Fig. 5(b)] compared to the thermal broadening of 300 K ≈ 30 meV.

D. Prototypical cases for larger Nernst coefficient

Although we obtained remarkably large $|N| \sim 20\ \mu$V/K in the above analysis, it is worth considering from wider perspective, so as to recognize different possibilities in other systems: Three prototypical cases (a)–(c) are listed in Table I, where different quantities are responsible for large $|N|$. We particularly set $|N| \gtrsim 10\ \mu$V/K as a typical target, which is close to the record-high experimental value [28], but an order of magnitude larger than the widely obtained experimental values $|N| < 1\ \mu$V/K.

An example of (c) is our previous finding [8], where the possibility of large $|N|$ was proposed within a single s-orbital model, which is much simpler than the present EuO model. While the considered spin texture was a common SkX, the behavior of TE coefficients was essentially different: There we found a striking peak of N around a specific band filling [29] where the large voltage mostly originates from pure ANE, i.e., large N_0. On the other hand, the present case is rather close to (b), where large $|r_H|$ is essential [30]. In whichever case, the presence of larger energy gaps in the electronic bands is generally desirable to achieve larger $|N|$ at higher temperatures (see the last paragraph of Sec. V C for a related example). In reality, however, $|N|$ remains rather small $\sim 1\ \mu$V/K in most of the materials whose TE coefficients have so far been measured, such that the situation is far from any of (a)–(c).

It would be particularly impressive if any material belonging to (c) is found, because it can be a good TE converter however small S_0 may be, i.e., something that has never been considered to be useful could belong to (c). When searching for its candidates, we can concentrate on the quantity α_{xy}, which is τ independent within the approximation of this study and can be compared between experiment and theory without worries about the delicate quantity τ and should first of all pursue larger α_{xy}.

E. Relevance to experiments

We comment on the feasibility of experimentally achieving the situation close to Fig. 5 and Fig. 6. The requirements are that (i) only about two conduction bands are occupied per skyrmion unit cell and that (ii) $\overline{\omega_s}\tau \gg 1$. These imply the following (i′) and (ii′), respectively, for a SkX with unit skyrmion that is assumed to be x times larger (in linear dimension) than ours (~ 1 nm): (i′) sheet electron density smaller at least by a factor of x^{-2} than our $\approx 10^{14}$ cm^{-2}, and (ii′) relaxation time τ longer at least by a factor of x^2 than our safe value 100 fs. For example, the experimental results on $LaAlO_3/SrTiO_3$ heterostructures of Ref. [31] satisfy both requirements for $x \sim 10$. While this system itself shows magnetism [32], systems of the same class but containing EuO layers, such as $LaAlO_3$/EuO [33] or $EuTiO_3$ [34], should better resemble our model and seem more promising, if carriers of similar quality, i.e., very dilute but mobile two-dimensional ones, can be induced.

F. Possibilities beyond our approximations

While we predict such a large Nernst coefficient as described in the previous section, there is some physics which is not captured in our theoretical formalism but could affect our results. It is roughly categorized into (i) electron-electron correlation effects beyond GGA+U approximation and (ii) scattering effects by disorder beyond constant RTA.

Next step regarding (i) would be to employ dynamical mean field theory [35] or GW approximation [36], which describe dynamical correlations in local and nonlocal levels, respectively. One of their consequences is to renormalize the band dispersion, modifying the Fermi-energy dependence of conductivity tensors $\tilde{\sigma}$ and $\tilde{\alpha}$, finally affecting the Nernst coefficient.

One possible next step regarding (ii) is to look for numerically exact solutions of the Boltzmann equation. In the equation, the scattering potential can most simply be modeled as some analytic function [37], but one can go further to extract it *ab initio* [38]. From the resulting distribution function, one can obtain not only the σ_{xx} modified from that within RTA [37] but also scattering-driven contributions $\sigma_{xy}^{\text{scatt.}}$ to the transverse components [38]. There is another possible way to evaluate *partial* contributions to $\sigma_{xy}^{\text{scatt.}}$. It is based on the formalism proposed in Ref. [39], which replaces the conventional Berry curvature Ω to $\Omega_{\text{disord.}}$ including the disorder effect. Such $\Omega_{\text{disord.}}$ can be obtained by first calculating the electronic structure of an *extended* unit cell, which is *disordered* as compared to the assumed primitive cell, and then unfolding the conventional $\Omega^{(\text{SBZ})}$ defined in the *shrunk* Brillouin zone onto the primitive zone. The difference of $\Omega_{\text{disord.}}$ and the conventional Ω in the primitive zone sums up to partially constitute $\sigma_{xy}^{\text{scatt.}}$ [39].

VI. SUMMARY & CONCLUSIONS

We showed from first principles that a very large Nernst coefficient $|N| \sim 20\ \mu$V/K would appear in the presence of skyrmion crystal magnetic order on a EuO monolayer. This is expected when a small number of carriers are introduced on top of the nontrivial insulating phase with Chern number -2, realized by the skyrmion-driven emergent magnetic field. Experiments on very clean interfaces or thin films containing EuO layers would hopefully observe this effect. In view of future energy-saving applications, extensive studies are needed

to realize such a giant Nernst effect in a wide range of more easily accessible systems hosting stable phases of skyrmion crystal.

ACKNOWLEDGMENTS

The authors thank N. Nagaosa and R. Arita for their insightful comments on this study. This work was supported by Japan Society for the Promotion of Science (JSPS) KAKENHI Grant No. JP17J03672. This work was partly supported by a JSPS Grant-in-Aid for Scientific Research on Innovative Area, "Nano Spin Conversion Science" (Grants No. 15H01015 and No. 17H05180). This work was also partly supported by JSPS Grant-in-Aid for Scientific Research (No. 16K04875). The computations in this research were performed using the supercomputers at ISSP, University of Tokyo.

[1] Y. Sakuraba, Scr. Mater. **111**, 29 (2016).
[2] D. Xiao, M. Chang, and Q. Niu, Rev. Mod. Phys. **82**, 1959 (2010).
[3] H. Chen, Q. Niu, and A. H. MacDonald, Phys. Rev. Lett. **112**, 017205 (2014).
[4] M. Ikhlas, T. Tomita, T. Koretsune, M. Suzuki, N. Daisuke, R. Arita, Y. Otani, and S. Nakatsuji, Nat. Phys. **13**, 1085 (2017).
[5] J. Zhou, Q. F. Liang, H. Weng, Y. B. Chen, S. H. Yao, Y. F. Chen, J. Dong, and G. Y. Guo, Phys. Rev. Lett. **116**, 256601 (2016).
[6] Several mechanisms are known to generate noncoplanar structures: Dzyaloshinskii-Moriya interaction, which is a particular form of spin-orbit interaction arising in a system without inversion center, or the electron-electron Coulomb interaction in a system with trigonal or hexagonal lattice symmetry, where it effectively creates frustrated exchange interactions among spins [40,41].
[7] N. Nagaosa and Y. Tokura, Nat. Nanotech. **8**, 899 (2013).
[8] Y. Mizuta and F. Ishii, Sci. Rep. **6**, 28076 (2016).
[9] K. Hamamoto, M. Ezawa, and N. Nagaosa, Phys. Rev. B **92**, 115417 (2015).
[10] Y. Shiomi, N. Kanazawa, K. Shibata, Y. Onose, and Y. Tokura, Phys. Rev. B **88**, 064409 (2013).
[11] Y. Hirokane, Y. Tomioka, Y. Imai, A. Maeda, and Y. Onose, Phys. Rev. B **93**, 014436 (2016).
[12] Y. Ohuchi, Y. Kozuka, M. Uchida, K. Ueno, A. Tsukazaki, and M. Kawasaki, Phys. Rev. B **91**, 245115 (2015).
[13] A class of topologically nontrivial phase, characterized by Chern number $\mathcal{C}$, which is a topological invariant and determines a quantized conductivity of AHE as $\sigma_{xy} = \mathcal{C}(e^2/h)$. In the context of systems relevant to ours, such a phase has already been predicted in a series of EuO/GdN hetero films, where an essential role was played by strong spin-orbit interaction [42], instead of the assumed skyrmion structure in our case.
[14] See, for example, the description between Eqs. (1) and (2) of Ref. [8].
[15] P. Wachter, CRC Crit. Rev. Solid State Sci. **3**, 189 (1972).
[16] The general description with $\boldsymbol{\Omega}(\boldsymbol{k})$ in $\boldsymbol{k}$ space can be translated into real space picture, in the approximation of strong Hund's coupling, where the spin-frozen electrons feel real magnetic field $B_{\rm spin}$ [9,24].
[17] J. Schoenes and P. Wachter, Phys. Rev. B **9**, 3097 (1974).
[18] T. Ozaki, H. Kino, J. Yu, M. J. Han, N. Kobayashi, M. Ohfuti, F. Ishii, T. Ohwaki, H. Weng, and K. Terakura, http://www.openmx-square.org/.
[19] A. Mostofi, J. Yates, G. Pizzi, Y. Lee, and I. Souza, Comput. Phys. Commun. **185**, 2309 (2014).
[20] G. Pizzi, D. Volja, B. Kozinsky, M. Fornari, and N. Marzari, Comput. Phys. Commun. **185**, 422 (2014).
[21] See, for example, Eq. (2) of Ref. [8] for the evaluated mathematical expressions.
[22] H. Miyazaki, T. Ito, H. J. Im, S. Yagi, M. Kato, K. Soda, and S. Kimura, Phys. Rev. Lett. **102**, 227203 (2009).
[23] M. Arai and Y. Hatsugai, Phys. Rev. B **79**, 075429 (2009).
[24] B. Göbel, A. Mook, J. Henk, and I. Mertig, Phys. Rev. B **95**, 094413 (2017).
[25] H. Miyazaki, H. Im, K. Terashima, S. Yagi, M. Kato, K. Soda, T. Ito, and S. Kimura, Appl. Phys. Lett. **96**, 232503 (2010).
[26] For the semiclassical picture of band conduction to be valid, $\varepsilon_F \tau \gg 1$ is required, and therefore we should limit ourselves to $\varepsilon_F \gg 50(5)$ meV for $\tau = 10(100)$ fs. To discuss as large N as possible but safely enough, we specifically discuss $\mu \sim \pm 30$ meV.
[27] This temperature is well beyond T_c of EuO system, and thus we now talk about any assumed system with similar band structure and $T_c \gtrsim 300$ K.
[28] Y. Pu, D. Chiba, F. Matsukura, H. Ohno, and J. Shi, Phys. Rev. Lett. **101**, 117208 (2008).
[29] The band filling corresponds to ε_F close to a van Hove singularity. Drastic change of Chern numbers in the vicinity of such singularities has already been observed [23,24], which received a novel interpretation recently [43].
[30] The $|r_H| \sim 0.2$ is one order of magnitude larger than the typical largest value obtained in "bad metal" (localization) regime. See, for example, the discussion in Supporting Online Material of Ref. [44].
[31] Y. Xie, C. Bell, M. Kim, H. Inoue, Y. Hikita, and H. Hwang, Sol. Stat. Commun. **197**, 25 (2014).
[32] A. Brinkman, M. Huijben, V. M. Zalk, J. Huijben, U. Zeitler, J. Maan, W. Wiel, G. Rijnders, D. H. Blank, and H. Hilgenkamp, Nat. Mater. **6**, 493 (2007).
[33] Y. Wang, M. K. Niranjan, J. D. Burton, J. M. An, K. D. Belashchenko, and E. Y. Tsymbal, Phys. Rev. B **79**, 212408 (2009).
[34] K. Ahadi, L. Galletti, and S. Stemmer, Appl. Phys. Lett. **111**, 172403 (2017).
[35] A. Georges, G. Kotliar, W. Krauth, and M. J. Rosenberg, Rev. Mod. Phys. **68**, 13 (1996).
[36] F. Aryasetiawan and O. Gunnarsson, Rep. Prog. Phys. **61**, 237 (1998).
[37] D. I. Pikulin, C. Y. Hou, and C. W. J. Beenakker, Phys. Rev. B **84**, 035133 (2011).
[38] C. Herschbach, Ph.D. thesis, Martin-Luther-Universität Halle-Wittenberg, 2015.

[39] R. Bianco, R. Resta, and I. Souza, Phys. Rev. B **90**, 125153 (2014).
[40] C. D. Batista, S. Lin, S. Hayami, and Y. Kamiya, Rep. Prog. Phys. **79**, 084504 (2016).
[41] T. Okubo, S. Chung, and H. Kawamura, Phys. Rev. Lett. **108**, 017206 (2012).
[42] K. F. Garrity and D. Vanderbilt, Phys. Rev. B **90**, 121103 (2014).
[43] G. G. Naumis, Phys. Lett. A **380**, 1772 (2016).
[44] W. L. Lee, S. Watauchi, V. Miller, R. Cava, and N. Ong, Science **303**, 1647 (2004).